

Biochimica et Biophysica Acta, 507 (1978) 433–444
© Elsevier/North-Holland Biomedical Press

BBA 77943

CALCULATION OF PHASE DIAGRAMS FOR NON-IDEAL MIXTURES OF LIPIDS, AND A POSSIBLE NON-RANDOM DISTRIBUTION OF LIPIDS IN LIPID MIXTURES IN THE LIQUID CRYSTALLINE PHASE

A.G. LEE

Department of Biochemistry, School of Biochemical and Physiological Sciences, University of Southampton, Southampton, SO9 3TU (U.K.)

(Received July 29th, 1977)

Summary

An approach is presented which can simulate phase diagrams for binary mixtures of lipid molecules showing close agreement with experimental data and using a single parameter to describe the non-ideality of mixing in each phase. It is suggested that lipid mixtures form non-ideal mixtures in the liquid crystalline phase. Application of the theory of athermal solutions allows an estimate to be made of the relative distribution of like and unlike lipid molecules about a central lipid molecule.

Introduction

Phase diagrams have now been reported for a number of binary mixtures of lipids (reviewed in ref. 1.). Some of these appear to indicate immiscibility of the lipids in the solid (gel) phase, and have been discussed in terms of a separation of the lipids within the plane of the bilayer [2–5]. These phase separations have been directly visualized for some mixtures by electron microscopy [6,7]. However, these observations are probably of relatively little direct importance to an understanding of biological membranes, since the bulk of the lipid in biological membranes appears to be in the liquid crystalline phase. Of more importance therefore is an understanding of the mixing properties of lipids in the liquid crystalline phase. An important application of classical thermodynamics is in the determination of the conditions required for phases to coexist in a state of equilibrium. In a previous paper [2] it was shown how phase diagrams could be calculated for binary mixtures of lipids, assuming ideal mixing. For mixtures of two very similar lipids such as dimyristoyl phosphatidylcholine and dipalmitoyl phosphatidylcholine, the experimentally determined phase diagram was very similar to that calculated for ideal mixing. For mixtures of lipids differing in head groups or differing in fatty acyl chain length

by more than two carbon atoms, however, mixing was far from ideal. It is now shown that such phase diagrams can be reproduced very satisfactorily assuming non-ideal mixing and with a single parameter to describe the non-ideality in the liquid crystalline state and in the gel state. These results strongly suggest that the distribution of lipids in mixtures in the liquid crystalline state is non-ideal.

Theoretical Methods

For an ideal binary system the chemical potential μ of a component in the liquid phase is given by

$$\mu_A^{\text{ideal}} = \mu_A^0 + RT \ln x_A^{\text{liq}} \quad (1)$$

where μ_A^0 is the chemical potential in the standard state, x_A^{liq} is the mol fraction of A in the liquid and T is the temperature. If it is assumed that the two components are completely immiscible in the solid phase, then Eqn. 1 leads to the conventional equation for the depression of the freezing point,

$$\ln x_A^{\text{liq}} = \frac{\Delta H_A}{R} \left(\frac{1}{T_A} - \frac{1}{T} \right) \quad (2)$$

where T_A and ΔH_A are, respectively, the melting point and heat of melting of component A. When the two components of the mixture form ideal solutions in both the liquid and solid phases, then an equation of type 1 has to be written for the solid phase, and the analysis becomes more complex. The result is the following equation for the mol fraction of A in the liquid phase, x_A^{liq} ,

$$x_A^{\text{liq}} = \frac{1 - k_B e^{\Delta H_B/RT}}{k_A e^{\Delta H_A/RT} - k_B e^{\Delta H_B/RT}} \quad (3)$$

where

$$k_A = 1/e^{\Delta H_A/RT_A} \quad (4)$$

and

$$k_B = 1/e^{\Delta H_B/RT_B} \quad (5)$$

where T_B and ΔH_B are, respectively, the melting point and heat of melting of component B. The mol fraction of A in the solid phase at the same temperature T , is given by [1],

$$x_A^{\text{solid}} = x_A^{\text{liq}} k_A e^{\Delta H_A/RT} \quad (6)$$

These same equations have been derived by Seltz [8] using a graphical procedure.

For a non-ideal mixture, the equation for the chemical potential in terms of the molar Gibb's free energy G is,

$$\mu_A = G + (1 - x_A) \frac{\partial G^E}{\partial x_A} \quad (7)$$

It is convenient to write the molar Gibb's free energy as the sum of that of an

ideal mixture (G^{ideal}) plus an excess molar Gibb's free energy (G^E),

$$G = G^{\text{ideal}} + G^E \quad (8)$$

Eqn. 7 then gives,

$$\mu_A = \mu_A^{\text{ideal}} + G^E(1 - x_A) \frac{\partial G^E}{\partial x_A} \quad (9)$$

If the two components are completely immiscible in the solid phase then Eqn. 9 gives an expression equivalent to that of Eqn. 2, namely

$$\ln x_A^{\text{liq}} = \frac{\Delta H_A}{R} \left(\frac{1}{T_A} - \frac{1}{T} \right) - \frac{1}{RT} \left[G^E + (1 - x_A^{\text{liq}}) \frac{\partial G^E}{\partial x_A^{\text{liq}}} \right] \quad (10)$$

If mixing had been ideal in the liquid phase, then this same mol fraction of A would have occurred at some other temperature T^{ideal} given from Eqn. 2 as

$$\ln x_A^{\text{liq}} = \frac{\Delta H_A}{R} \left(\frac{1}{T_A} - \frac{1}{T^{\text{ideal}}} \right) \quad (11)$$

Subtracting Eqn. 11 from Eqn. 10 gives

$$\frac{1}{RT} \left[G^E + (1 - x_A^{\text{liq}}) \frac{\partial G^E}{\partial x_A^{\text{liq}}} \right] = \frac{\Delta H_A}{R} \left(\frac{1}{T^{\text{ideal}}} - \frac{1}{T} \right) \quad (12)$$

For many binary systems, the excess molar Gibb's free energy can be approximated by [9]

$$\begin{aligned} G^E &= \rho_0 x_A^{\text{liq}} \cdot x_B^{\text{liq}} \\ &= \rho_0 x_A^{\text{liq}} \cdot (1 - x_A^{\text{liq}}) \end{aligned} \quad (13)$$

where ρ_0 is a constant which characterizes the solution behaviour. Substitution of Eqn. 13 into Eqn. 12 gives

$$\frac{\rho_0(1 - x_A^{\text{liq}})^2}{\Delta H_A} = \frac{T}{T^{\text{ideal}}} - 1 \quad (14)$$

This equation then allows the calculation of phase diagrams, taking into account deviations from ideality in the liquid phase.

The corresponding calculation for binary mixtures where both solid and liquid phases from non-ideal solutions is considerably more complicated. In this case, expressions like Eqn. 9 have to be written for both the solid and the liquid phases. The required expressions that are obtained are [1],

$$\begin{aligned} \ln \left(\frac{x_A^{\text{liq}}}{x_A^{\text{solid}}} \right) &+ \frac{\rho_0^{\text{liq}}(1 - x_A^{\text{liq}})^2 - \rho_0^{\text{solid}}(1 - x_A^{\text{solid}})^2}{RT} \\ &= \frac{\Delta H_A}{R} \left(\frac{1}{T_A} - \frac{1}{T} \right) \end{aligned} \quad (15)$$

and

$$\ln \left(\frac{1 - x_A^{\text{liq}}}{1 - x_A^{\text{solid}}} \right) + \frac{\rho_0^{\text{liq}}(x_A^{\text{liq}})^2 - \rho_0^{\text{solid}}(x_A^{\text{solid}})^2}{RT} = \frac{\Delta H_B}{R} \left(\frac{1}{T_B} - \frac{1}{T} \right) \quad (16)$$

Because of their transcendental nature, Eqns. 15 and 16 require numerical methods for their solution (either a simple iteration technique or the Newton-Raphson technique).

As will be seen, the equations presented here provide a suitable procedure for fitting the experimentally observed phase diagrams.

Information about the non-ideal mixing of the lipids is contained in the parameter ρ_0 , and it is now necessary to consider in more detail the meaning of this parameter. The excess molar Gibb's free energy consists of two parts, an excess enthalpy and an excess entropy,

$$G^E = H^E - TS^E \quad (17)$$

The simplest model for a solution is to assume that G^E is zero, in which case one obtains an ideal solution. The next simplest assumption is to put either H^E or S^E to zero. The first assumption that H^E is zero leads to the concept of athermal solutions and the second assumption that S^E is zero leads to the concept of regular solutions [9]. Both approaches are, of course, over simplifications, but they have led to the development of interesting ideas in solution chemistry. In particular, the athermal solution model has attracted much attention [9]. In this paper, I will show the consequences of assuming an athermal solution model for lipid mixtures.

In the athermal solution model all the non-ideality of mixing is attributed to a non-random distribution of molecules. Wilson [10] considered a central molecule of type A in a binary mixture, where the probability of finding a molecule of type B next to this central molecule compared to the probability of finding a molecule of type A is given by

$$\frac{x_{AB}}{x_{AA}} = \frac{x_B \exp - [E_{AB}/RT]}{x_A \exp - [E_{AA}/RT]} \quad (18)$$

Here E_{AB} and E_{AA} are proportional to the A-B and A-A interaction energies, respectively. Thus this equation simply states that the ratio of the amounts of B and A molecules around a central A molecule is equal to the ratio of the mol fraction of B and A weighted statistically by the two Boltzmann factors.

In the Flory-Huggins theory for athermal mixtures [11]

$$G^E = RT \sum_{i=1}^{\infty} x_i \ln \frac{\phi_i}{x_i} \quad (19)$$

where ϕ_i is the volume fraction of i and x_i is the mol fraction of i . Wilson [10] empirically redefined these volume fractions in terms of so-called local volume fractions f_A and f_B ,

$$f_A = \frac{x_A \nu_A \exp - [E_{AA}/RT]}{x_A \nu_A \exp - [E_{AA}/RT] + x_B \nu_B \exp - [E_{AB}/RT]} \quad (20)$$

and

$$f_B = \frac{x_B \nu_B \exp - [E_{BB}/RT]}{x_B \nu_B \exp - [E_{BB}/RT] + x_A \nu_A \exp - [E_{AB}/RT]} \quad (21)$$

where ν_A and ν_B are the molar volumes of pure A and B, respectively. Defining

$$F_{AB} = \frac{\nu_B}{\nu_A} \exp - [(E_{AB} - E_{AA})/RT] \quad (22)$$

and

$$F_{BA} = \frac{\nu_A}{\nu_B} \exp - [(E_{AB} - E_{BB})/RT] \quad (23)$$

and substituting into Eqn. 19, we obtain the Wilson equation for a binary mixture

$$\frac{G^E}{RT} = -x_A \ln(x_A + F_{AB}x_B) - x_B \ln(F_{BA}x_A + x_B) \quad (24)$$

For the case of the lipid molecules considered here, it is reasonable to put $\nu_A = \nu_B$. In the case where Eqn. 13 can be used to obtain a good fit to the experimental data, then comparison of Eqns. 13 and 24, show that, for reasons of symmetry,

$$F_{AB} = F_{BA} \quad (25)$$

It further follows that when $x_A = x_B = \frac{1}{2}$,

$$\frac{\rho_0}{4RT} = -\ln\left(\frac{1}{2} + \frac{F_{AB}}{2}\right) \quad (26)$$

The value of ρ_0 that gives the best fit to the experimental data can therefore be used to obtain the value of F_{AB} and hence from Eqn. 18, the relative distributions of the lipids.

Results

Before any attempt can be made to fit experimental phase diagrams to those calculated theoretically, some account has to be taken of the finite width of the experimental phase diagram. The Gibbs phase rule, on which the concept of the phase diagram is based, applies only to discontinuous phase transitions occurring sharply at a single temperature. For lipids, although the phase transition is first order as shown by a latent heat of transition, the transition takes place over a significant temperature range. Mabrey and Sturtevant [12] have corrected for the finite width of the phase transition by assuming that part of the separation in temperature for the onset and completion of gel phase formation for lipid mixtures is due to the finite width of the transition for the component lipids. They then assume that this contribution is given by the weighted average of the contributions from the component lipids and that subtraction will therefore give temperatures which can be more truly plotted as a phase diagram. Although there is no obvious theoretical justification for this ap-

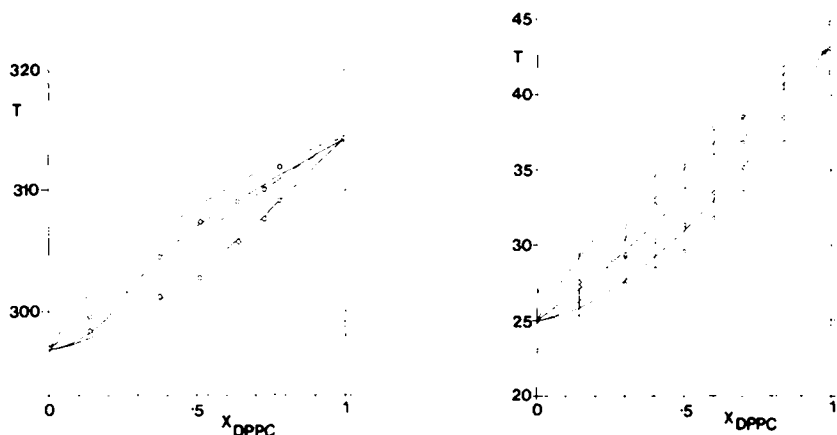


Fig. 1. Phase diagram for mixtures of dimyristoyl phosphatidylcholine and dipalmitoyl phosphatidylcholines. Circles, corrected points determined calorimetrically (from ref. 12). Broken lines, phase diagram calculated for ideal mixing in the liquid and solid phases. Solid lines, transition curves calculated for non-ideal mixing in the liquid and solid phases (parameters given in Table I). Temperatures in K.

Fig. 2. Phase diagram for mixtures of dimyristoyl phosphatidylcholine and dipalmitoyl phosphatidylcholine. Circles, corrected and uncorrected points determined calorimetrically (from ref. 13). Broken lines, phase diagram calculated for ideal mixing in the liquid and solid phases. Solid lines, phase diagram calculated for non-ideal mixing in the liquid and solid phases (parameters given in Table I). Temperatures in °C.

proach, it seems to be the best available, and will be adopted here. It means however that there will be a certain indeterminacy in any attempt to fit experimental and theoretical data.

Fig. 1 shows the phase diagram obtained calorimetrically for mixture of dimyristoyl phosphatidylcholine and dipalmitoyl phosphatidylcholine [12] and

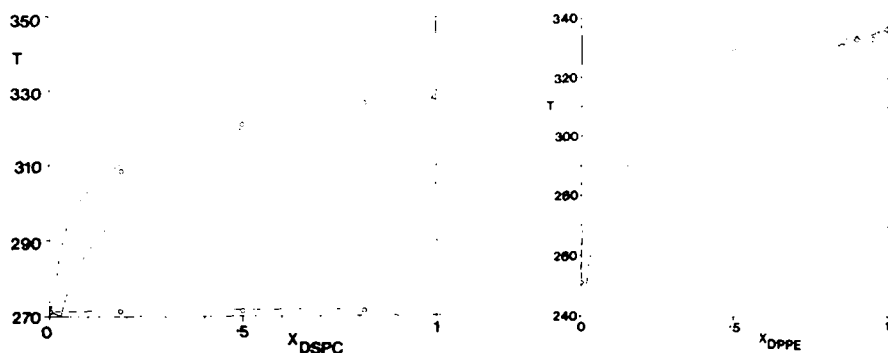


Fig. 3. Phase diagram for mixtures of dilauroyl phosphatidylcholine and distearoyl phosphatidylcholine. Circles, corrected points determined calorimetrically (from ref. 12). Solid lines, phase diagram calculated for ideal mixing in the liquid phase. Broken lines, phase diagram calculated for non-ideal mixing in the liquid phase. Temperatures in K.

Fig. 4. Phase diagram for mixtures of dioleoyl phosphatidylcholine and dipalmitoyl phosphatidylethanolamine. Circles, points determined by electron spin resonance (from ref. 3). Solid lines, phase diagram calculated for ideal mixing in the liquid phase. Broken lines, phase diagram calculated for non-ideal mixing in the liquid phase. Temperatures in K.

corrected as described above. The experimentally obtained diagram is very similar to that calculated from Eqns. 3 and 6 assuming ideal mixing in both the solid and liquid phases [2] using the transition data from ref. 12. The data can be fitted better, however, by assuming non-ideal mixing in both phases, as shown in Fig. 1 for the curves calculated from Eqns. 15 and 16 with $\rho_0^{\text{liq}} = 550$ cal/mol and $\rho_0^{\text{solid}} = 950$ cal/mol. Fig. 2 shows a fit to the phase diagram for the same system obtained by Blume and Ackermann [13], using their transition data. Fig. 3 shows the phase diagram obtained calorimetrically for mixtures of dilauroyl phosphatidylcholine and distearoyl phosphatidylcholine [12]. Clearly, the two components are essentially immiscible in the solid phase, but the fit of the liquidus curve to Eqn. 2 is relatively poor. However, an excellent fit is obtained to Eqn. 14 assuming non-ideal mixing in the liquid phase with $\rho_0 = 0.71$ kcal/mol.

Fig. 4 shows the agreement that can be obtained between the model involving non-ideal mixing and the experimental data for the dioleoyl phosphatidylcholine-dipalmitoyl phosphatidylethanolamine system obtained using an electron spin resonance probe [3]. For mixtures of dimyristoyl phosphatidylcholine and distearoyl phosphatidylcholine, there is disagreement as to whether or not the two components are immiscible in the solid state [4,12]. In Fig. 5 the data from the experiments using an electron spin resonance probe are used [4], assuming immiscibility in the solid phase.

Fig. 6 shows an attempt to fit the phase diagram for mixtures of dimyristoyl phosphatidylcholine and dimyristoyl phosphatidylethanolamine. Although agreement is not very good, the diagram calculated for non-ideal mixing is at least closer to reproducing the width of the diagram, than is that calculated for ideal mixing.

Figs. 7 and 8 show the data obtained by Mabrey and Sturtevant [12] and Blume and Ackermann [13] for mixtures of dimyristoyl phosphatidylethanol-

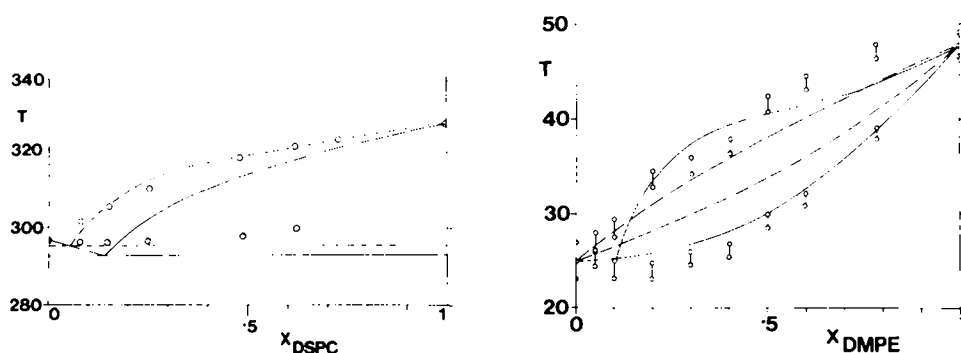


Fig. 5. Phase diagram for mixtures of dimyristoyl phosphatidylcholine and distearoyl phosphatidylcholine. Circles, points determined by electron spin resonance (from ref. 4). Solid lines, phase diagram calculated for ideal mixing in the liquid phase. Broken lines, phase diagram calculated for non-ideal mixing in the liquid phase.

Fig. 6. Phase diagram for mixtures of dimyristoyl phosphatidylcholine and dimyristoyl phosphatidylethanolamine. Circles, corrected and uncorrected points determined calorimetrically (from ref. 13). Broken lines, phase diagram calculated for ideal mixing. Solid lines, phase diagram calculated for non-ideal mixing (parameters in Table I). Temperatures in $^{\circ}\text{C}$.

TABLE I
PARAMETERS OBTAINED FROM AN ANALYSIS OF EXPERIMENTALLY OBTAINED PHASE DIAGRAMS

Lower melting component	Higher melting component	ρ_0^{liq} (kcal/mol)	ρ_0^{solid} (kcal/mol)	F_{AB}^{liq}	F_{AB}^{solid}	x_{AA}^{liq} x_{AB} at 1:1 molar ratio	x_{AA}^{solid} x_{AB} at 1:1 molar ratio
Dilauroyl phosphatidylcholine *	Distearoyl phosphatidylcholine	0.7	—	0.494	—	2.02	—
Dimyristoyl phosphatidylcholine **	Distearoyl phosphatidylcholine	0.7	—	0.494	—	2.02	—
Dioleoyl phosphatidylcholine ***	Dipalmitoyl phosphatidylethanolamine	1.25	—	0.188	—	5.32	—
Dimyristoyl phosphatidylcholine *	Dipalmitoyl phosphatidylcholine	0.55	0.95	0.590	0.346	1.69	2.89
Dimyristoyl phosphatidylcholine †	Dipalmitoyl phosphatidylcholine	0.5	0.9	0.618	0.366	1.62	2.73
Dimyristoyl phosphatidylethanolamine *	Distearoyl phosphatidylcholine	1.15	1.45	0.238	0.093	4.20	10.75
Dimyristoyl phosphatidylcholine †	Dimyristoyl phosphatidylethanolamine	1.0	1.5	0.309	0.090	3.24	11.11
Dimyristoyl phosphatidylethanolamine †	Distearoyl phosphatidylcholine	1.5	1.6	0.238	0.060	4.20	16.67

* Data from ref. 12.

** Data from ref. 4.

*** Data from ref. 3.

† Data from ref. 13.

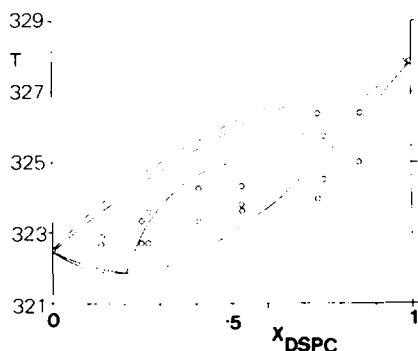


Fig. 7. Phase diagram for mixtures of dimyristoyl phosphatidylethanolamine and distearoyl phosphatidylcholine. Circles, corrected points determined calorimetrically (from ref. 12). Broken lines, phase diagram calculated for ideal mixing in liquid and solid phases. Solid lines, phase diagram calculated for non-ideal mixing in the liquid and solid phases.

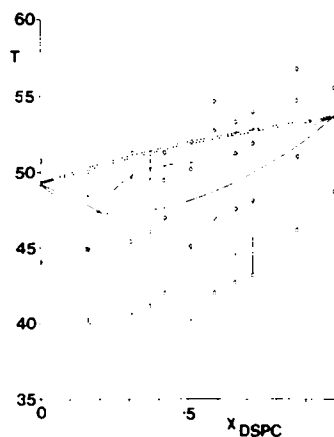


Fig. 8. Phase diagram for mixtures of dimyristoyl phosphatidylethanolamine and distearoyl phosphatidylcholine. Circles, corrected and uncorrected points determined calorimetrically (from ref. 13). Broken lines, phase diagram calculated for ideal mixing. Solid lines, phase diagram calculated for non-ideal mixing (parameters in Table I). Temperatures in °C.

amine and distearoyl phosphatidylcholine. Agreement between the experimental data is not very good, probably attributable to the large contribution to the width of the phase transition for the mixtures attributable to the finite widths for the transitions of the component lipids. However, it is easily possible to obtain a phase diagram for non-ideal mixing which is closer to the experimental data than that obtained assuming ideal mixing. As described elsewhere [1] the shapes of the calculated phase diagrams are very sensitive to the values of ρ_0 , and variation of ρ_0 by more than ± 0.1 kcal/mol produces an appreciably worse fit to the data.

No attempt has been made to fit the experimentally obtained phase diagram for mixtures of dipalmitoyl phosphatidylcholine and dipalmitoyl phosphatidylethanolamine [13]. The data obtained calorimetrically shows a minimum in the solidus curve, which does not appear in the phase diagrams obtained for the same mixtures using electron spin resonance [4] or fluorescence [2] techniques. The presence of such a minimum has a large effect on the values of ρ_0 required to give a good fit to the data.

The ρ_0 values obtained from these analyses are listed in Table I. From these values, values of F_{AB} can be obtained from Eqn. 26 and so values for the ratio x_{AB}/x_{AA} at a 1 : 1 molar ratio. For the range of ρ_0 values reported here, the values of the excess Gibbs free energy G^E calculated by Eqns. 13 and 24 agree to within better than 10%.

Discussion

In previous papers, discussion of lipid phase diagrams has centred around possible immiscibility for lipids in the gel phase, with consequent lateral phase

separations [2–5]. Important though these discussions are, of more importance to an understanding of the structure of biological membranes is an understanding of the mixing properties of lipids in the liquid crystalline phase, since the bulk of the lipids in a biological membrane appear to be in such a phase [5]. Here we show that published phase diagrams can be analysed to give information about mixing in the liquid crystalline phase.

Reasonably good agreement between theoretical and experimental phase diagrams can be obtained assuming either non-ideal mixing in the liquid crystalline phase and complete immiscibility in the gel phase, or non-ideal mixing in both phases, depending on the lipid mixtures. The agreement is particularly impressive since it involves a single non-ideality parameter for each phase. One major limitation to the goodness-of-fit that can be obtained is provided by problems associated with the finite width of lipid phase transitions.

As would be expected, the value of the non-ideality parameter ρ_0 in the liquid crystalline phase increases with increasing dissimilarity between the lipids, whether caused by differences in fatty acyl chains or lipid head group. Also as might have been expected the values of ρ_0 for the gel phase are greater than those in the liquid crystalline phase, for some mixtures leading to complete immiscibility.

The generally good agreement between experiment and theory gives some grounds for confidence in the reality of the values of the parameter ρ_0 describing the non-ideality of mixing. If heats of mixing were known for lipids, then it would be possible to obtain entropies of mixing for the lipids from ρ_0 , and so estimates of the randomness of mixing. Unfortunately, heats of mixing have not been determined. A similar problem arises in studies of many other liquid mixtures, and has led to the adoption of one of two relatively simple models for the behaviour of mixtures, either that of athermal mixtures or that of regular mixtures [9]. Both are obvious over-simplifications but the former has been shown to be useful in the understanding of other liquid mixtures. By attributing all the non-ideality of mixing to the entropy term, the extent of non-random mixing will probably be exaggerated. On the other hand, in the regular solution model, all the non-ideality of mixing is attributed to the enthalpy term, and a random distribution of the two components of the mixture is assumed. However, as Hildebrand and Scott [14] comment: "We have seen that a non-zero energy of mixing must be attributed to differences in the interaction potential of 1-1 pairs, 2-2 pairs and 1-2 pairs. It is evident however, that such a difference in the interaction energy must lead to a degree of preferential formation of either unlike pairs (1-2) or like pairs (1-1 and 2-2). To the extent that such a preferential order exists, our calculations of the entropy and the energy of mixing both of which assumed no such order, are in error."

In the absence of heat of mixing data, it is therefore of some interest to explore the consequences of the athermal model. The fact that the values of the parameter F_{AB} are positive for all the lipid mixtures studied here (Table I) means that the energy of interaction between two like molecules is more negative (i.e. stronger) than the energy of interaction between two unlike molecules. Differences are, however, quite small, as can be seen if values for E_{AA} are estimated for lipids in a bilayer. This can be done since the energy of interaction between two like molecules is given approximately by (ref. 15),

$$E_{AA} = -\frac{2}{z}(\Delta H_v - RT) \quad (27)$$

where ΔH_v is the latent heat of vaporization and z is the liquid phase co-ordination number, assumed to be 6 in this case. Although the enthalpy of vaporization of a lipid molecule is unknown, the enthalpies of vaporization of 1-hexadecane and 1-hexadecanoic acid have been determined to be 30 and 37 kcal/mol, respectively [16,17]. Taking the figure of 37 kcal/mol as a lower limit for the enthalpy of vaporization of the lipid, E_{AA} can be estimated to be more negative than ca -12.1 kcal/mol. Then for mixtures of dimyristoyl and distearoyl phosphatidylcholine, for example, E_{AB} would be approx. -11.7 kcal/mol. This very small difference, however, can have a very significant effect on the distribution of lipid molecules within the bilayer in the liquid crystalline phase. Fig. 9 shows the relative distribution of like and unlike lipids around a central lipid, for various mol fractions of the two lipids in the bilayer.

Although these non-random distributions will probably be over estimates because of the assumptions of the athermal mixing model, they do very strongly suggest that a non-random distribution of lipids can be expected even in lipid bilayers in the liquid crystalline phase. The only previous suggestions for a non-random distribution of this type appear to be in mixtures of dielaidoyl phosphatidylcholine and dipalmitoyl phosphatidylethanolamine [3] and the possible preferential interaction of cholesterol with unsaturated lipid molecules in mixture of saturated and unsaturated lipids [18,19].

The reason why the average energy of interactions between two phosphatidylcholine molecules with the same fatty acyl chains is higher than that between two phosphatidylcholine molecules with different fatty acyl chains is probably connected with the mismatch in packing that will occur between chains of different length. Some evidence for this has been found in previous measurements of ^{13}C nuclear magnetic resonance relaxation times (Table II). In mixtures of dioleoyl phosphatidylcholine and dipalmitoyl phosphatidylcholine in the liquid crystalline phase there is an increase in relaxation times at the terminal methyl ends of the fatty acyl chains over those in the pure lipids. This is equivalent to an increased rate of motion about C-C bonds at the methyl end of the chains [20], and can be attributed to the formation of void volume at the centre of the bilayer due to the differences in fatty acyl chain length.

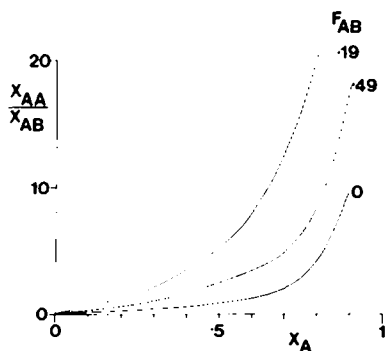


Fig. 9. The distribution ratio x_{AA}/x_{AB} vs. mol fraction of A, for various values of the parameter F_{AB} .

TABLE II

 ^{13}C T_1 RELAXATION IN AQUEOUS SONICATED LIPID DISPERSIONS AT 52°C

Data from ref. 20 and Birdsall, N.J.M., Lee, A.G., Metcalfe, J.C. and Warren, G.B., unpublished observations.

Carbon	T_1 (s)		
	Dipalmitoyl phosphatidylcholine	Dioleoyl phosphatidylcholine	Dioleoyl phosphatidylcholine plus dipalmitoyl phosphatidyl- choline, 1 : 2 molar ratio
Choline NMe ₃ ⁺	0.70 ± 0.03	1.06 ± 0.06	0.74 ± 0.05
Chain C ₃	0.22 ± 0.03	0.26 ± 0.12	0.29 ± 0.02
(CH ₂) _n	0.53 ± 0.01	0.73 ± 0.03	0.54 ± 0.01
C _{14,16}	1.13 ± 0.18	1.38 ± 0.16	1.90 ± 0.30
C _{15,17}	1.81 ± 0.08	2.26 ± 0.11	2.45 ± 0.08
C _{15,18}	3.34 ± 0.25	3.88 ± 0.37	4.40 ± 0.54

References

- 1 Lee, A.G. (1977) *Biochim. Biophys. Acta* 472, 285–344
- 2 Lee, A.G. (1975) *Biochim. Biophys. Acta*, 413, 11–23
- 3 Wu, S.H. and McConnell, H.M. (1975) *Biochemistry* 14, 847–854
- 4 Shimshick, E.J. and McConnell, H.M. (1973) *Biochemistry* 12, 2351–2360
- 5 Lee, A.G. (1975) *Prog. Biophys. Mol. Biol.* 29, 3–56
- 6 Ververgaert, P.H.J. Th., Verkleij, A.J., Elbers, P.F. and van Deenen, L.L.M. (1973) *Biochim. Biophys. Acta* 311, 320–329
- 7 Grant, C.W.M., Wu, S.H. and McConnell, H.M. (1974) *Biochim. Biophys. Acta* 363, 151–158
- 8 Seltz, H. (1934) *J. Am. Chem. Soc.* 56, 307–311
- 9 Eckert, C.A. (1976) in *Solutions and Solubilities* (Dack, M.R.J., ed.), Part II, Wiley, New York
- 10 Wilson, G.M. (1964) *J. Am. Chem. Soc.* 86, 127–130
- 11 Flory, P.J. (1942) *J. Chem. Phys.* 10, 51–61
- 12 Mabrey, S. and Sturtevant, J.M. (1976) *Proc. Natl. Acad. Sci. U.S.* 73, 3862–3866
- 13 Blume, A. and Ackermann, T. (1974) *FEBS Lett.* 43, 71–74
- 14 Hildebrand, J.H. and Scott, R.L. (1950) *The Solubility of Nonelectrolytes*, pp. 134–135, Reinhold Publ. Co., New York
- 15 Wong, K.F. and Eckert, C.A. (1971) *Ind. Eng. Chem. Fundam.* 10, 20–23
- 16 Bradley, R.S. and Shellard, A.D. (1949) *Proc. R. Soc. London, Ser. A* 198, 239–251
- 17 Davies, M. and Malpass, V.E. (1961) *J. Chem. Soc.* 1048–1055
- 18 de Kruffy, B., Demel, R.A., Stotboom, J.A., van Deenen, L.L.M. and Rosenthal, A.F. (1973) *Biochim. Biophys. Acta* 307, 1–19
- 19 Lee, A.G. (1976) *FEBS Lett.* 62, 359–363
- 20 Levine, Y.K., Birdsall, N.J.M., Lee, A.G. and Metcalfe, J.C. (1972) *Biochemistry* 11, 1416–1421